

## Recent Advances in Sensitized Mesoscopic Solar Cells

MICHAEL GRÄTZEL\*

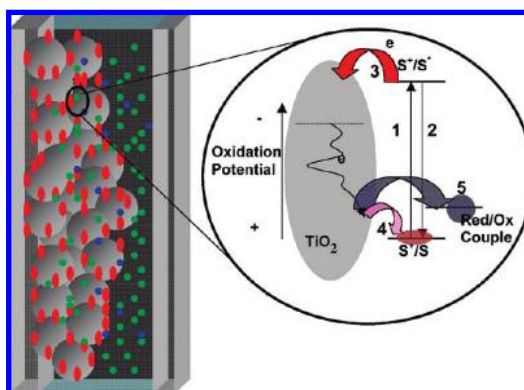
*Laboratory of Photonics and Interfaces, Institute of Chemical Science and Engineering, Faculty of Basic Science, Ecole Polytechnique Fédérale de Lausanne, CH-1015 Lausanne, Switzerland*

RECEIVED ON MAY 3, 2009

### CONSPECTUS

Perhaps the largest challenge for our global society is to find ways to replace the slowly but inevitably vanishing fossil fuel supplies by renewable resources and, at the same time, avoid negative effects from the current energy system on climate, environment, and health. The quality of human life to a large degree depends upon the availability of clean energy sources. The worldwide power consumption is expected to double in the next 3 decades because of the increase in world population and the rising demand of energy in the developing countries. This implies enhanced depletion of fossil fuel reserves, leading to further aggravation of the environmental pollution. As a consequence of dwindling resources, a huge power supply gap of 14 terawatts is expected to open up by year 2050 equaling today's entire consumption, thus threatening to create a planetary emergency of

gigantic dimensions. Solar energy is expected to play a crucial role as a future energy source. The sun provides about 120 000 terawatts to the earth's surface, which amounts to 6000 times the present rate of the world's energy consumption. However, capturing solar energy and converting it to electricity or chemical fuels, such as hydrogen, at low cost and using abundantly available raw materials remains a huge challenge. Chemistry is expected to make pivotal contributions to identify environmentally friendly solutions to this energy problem. One area of great promise is that of solar converters generally referred to as "organic photovoltaic cells" (OPV) that employ organic constituents for light harvesting or charge carrier transport. While this field is still in its infancy, it is receiving enormous research attention, with the number of publications growing exponentially over the past decade. The advantage of this new generation of solar cells is that they can be produced at low cost, i.e., potentially less than 1 U.S. \$/peak watt. Some but not all OPV embodiments can avoid the expensive and energy-intensive high vacuum and materials purification steps that are currently employed in the fabrication of all other thin-film solar cells. Organic materials are abundantly available, so that the technology can be scaled up to the terawatt scale without running into feedstock supply problems. This gives organic-based solar cells an advantage over the two major competing thin-film photovoltaic devices, i.e., CdTe and CuIn(As)Se, which use highly toxic materials of low natural abundance. However, a drawback of the current embodiment of OPV cells is that their efficiency is significantly lower than that for single and multicrystalline silicon as well as CdTe and CuIn(As)Se cells. Also, polymer-based OPV cells are very sensitive to water and oxygen and, hence, need to be carefully sealed to avoid rapid degradation. The research discussed within the framework of this Account aims at identifying and providing solutions to the efficiency problems that the OPV field is still facing. The discussion focuses on mesoscopic solar cells, in particular, dye-sensitized solar cells (DSCs), which have been developed in our laboratory and remain the focus of our investigations. The efficiency problem is being tackled using molecular science and nanotechnology. The sensitizer constitutes the heart of the DSC, using sunlight to pump electrons from a lower to a higher energy level, generating in this fashion an electric potential difference, which can be exploited to produce electric work. Currently, there is a quest for sensitizers that achieve effective harnessing of the red and near-IR part of sunlight, converting these photons to electricity better than the currently used generation of dyes. Progress in this area has been significant over the past few years, resulting in a boost in the conversion efficiency of the DSC that will be reviewed.



## Introduction

Following their inception in 1985,<sup>1–6</sup> dye-sensitized mesoscopic solar cells (DSCs) are often included in the organic photovoltaic (OPV) family because of the organic nature of at least part of its constituents. The DSC is the only photovoltaic device that uses molecules to absorb photons and convert them to electric charges without the need of intermolecular transport of electronic excitation. It is also the only solar cell that separates the two functions of light harvesting and charge-carrier transport, whereas conventional and all of the other known OPV devices perform both operations simultaneously. This imposes stringent demands upon the optical and electronic properties of the semiconductor, i.e., its band gap and band position, as well as charge-carrier mobility and the recombination time of photogenerated charges, restricting greatly the choice of suitable materials that are able to act as efficient photovoltaic converters. The separation of light absorption and carrier transport on the other hand opens up a vast amount of options for the absorber material. The molecular sensitizer or semiconductor quantum dot is placed at the interface between an electron (n) and hole (p) conducting material (Figure 1). The former is typically a wide band semiconductor oxide, such as TiO<sub>2</sub>, ZnO, or SnO<sub>2</sub>, while the latter is a redox electrolyte or a p-type semiconductor. Upon photo-excitation, the sensitizer injects an electron in the conduction band of the oxide and is regenerated by hole injection in the electrolyte or p-type conductor. Alternatively, the sensitizer

may be attached to a p-type oxide, such as NiO,<sup>7</sup> which in this case reduces the excited dye, with the latter being regenerated from its reduced form by electron transfer to an acceptor in the electrolyte. In both cases, the role of the sensitizer is to absorb light and generate positive- and negative-charge carriers.

Note that minority carriers, i.e., electrons and positive charges (holes) in p- and n-doped semiconductors, respectively, play no role in the photovoltaic conversion process accomplished by the DSC. Because the sensitizer injects electrons in the n-type and holes in the p-type collector, only majority carriers are generated. These charges move in their respective transport medium to the front and back contacts of the photocell, where they are collected as electric current. In contrast, in conventional p–n junction photovoltaic cells, the photocurrent arises from minority carriers generated by photo-excitation of the semiconductor. The minority carrier must live long enough to reach the junction formed between the p- and n-doped semiconductor material before recombination with the majority carriers takes place. The electric field present in the vicinity of the junction separates the positive and negative charges generated under illumination, attracting the electrons to the n-doped and the holes to the p-doped material. To impart a sufficiently long lifetime to the photogenerated electron–hole pairs, the use of very pure materials is required. The chemical purification of the semiconductor entails a high cost for the photovoltaic converter.

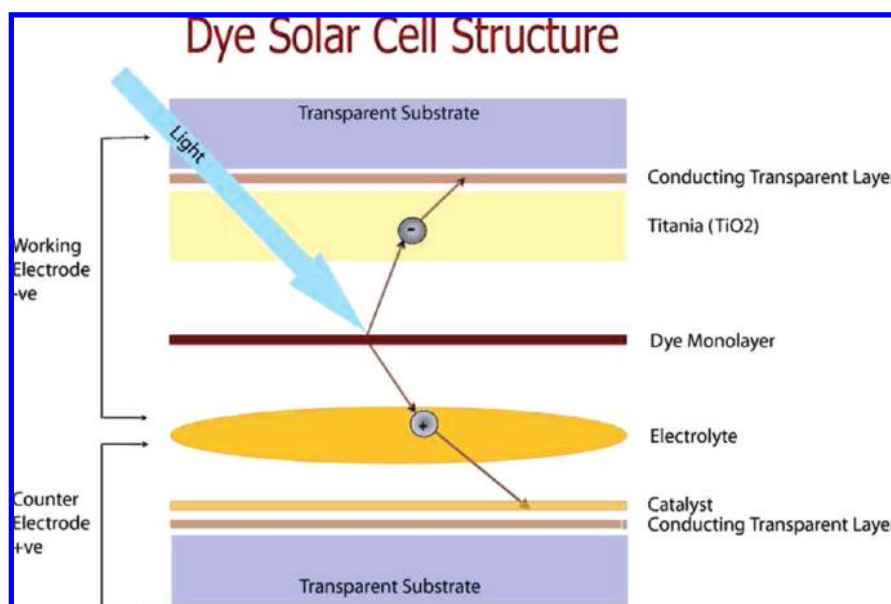


**FIGURE 1.** Schematic illustration of the operation principle for molecular photovoltaic cell. The heart of the device is a sensitizer placed at the interface between an electron (n) and hole (p) conducting material. Upon photo-excitation, it injects an electron in the conduction band of a wide band gap semiconducting oxide and is regenerated by hole injection in a redox electrolyte or p-type conductor. The charges diffuse to the front and back contact, where they generate an electric current. The open circuit photovoltage corresponds to the difference in the Fermi level of the n- and p-type conductor under illumination.

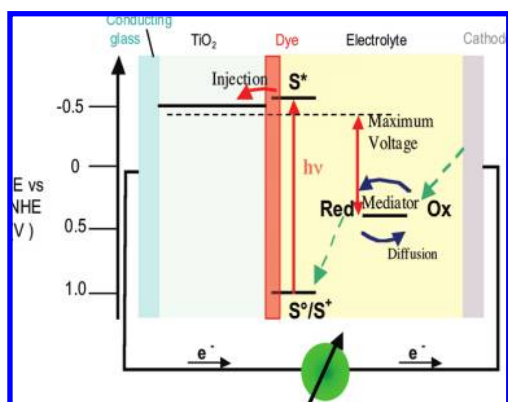


**FIGURE 2.** Energy band diagram of a typical embodiment of the DSC employing an iodide/triiodide-based redox electrolyte and N719 as a sensitizer.

In the DSC, the recombination of charge carriers occurs across the phase boundary separating the electron from the hole conductor medium. This inherent geometry offers the unique prospective to fashion the interface in a judicious manner to retard the back-electron-transfer reaction. One promising approach to accomplish this goal is the molecular engineering of sensitizers forming a self-assembled compact monolayer alone or in conjunction with a co-adsorbent at the oxide surface. Such an insulating film would impair the flow of dark current across the junction, reducing the back-reaction rate and increasing the overall solar to electric power conversion efficiency of the cell.

Figure 2 shows a typical band diagram of the DSC. Sunlight is harvested by the sensitizer that is attached to the surface of a large band gap semiconductor, typically a film constituted of titania nanoparticles. Photo-excitation of the dye results in the injection of electrons into the conduction band of the oxide. The dye is regenerated by electron donation from an organic hole conductor or an electrolyte that is infiltrated into the porous films. The latter contains, most frequently, the iodide/triiodide couple as a redox shuttle, although other mediators, such as cobalt(II/III) complexes<sup>8,9</sup> or the TEMPO/TEMPO<sup>+</sup> redox couple,<sup>10</sup> have also been developed recently as an alternative to the I<sup>-</sup>/I<sub>3</sub><sup>-</sup> system. Reduction of S<sup>+</sup> by iodide regenerates the original form of the dye while producing triiodide ions. This prevents any significant buildup of S<sup>+</sup>, which could recapture the conduction band electron at the surface. The iodide is regenerated in turn by the reduction of the triiodide ions at the counter-electrode, where the electrons are supplied via migration through the external load completing the cycle. Thus, the device is generating electricity from light without any permanent chemical transformation. The voltage produced under illumination corresponds to the difference between the chemical potential (Fermi level),

$\mu(e^-)$ , that the electrons attain in the titania nanoparticles and the chemical potential  $\mu(h^+)$  of the holes in the hole conductor. For redox electrolytes, the latter corresponds to the Nernst potential. Note that, in the dark at equilibrium,  $\mu(e^-) = \mu(h^+)$ , i.e., the Fermi level, is constant within the whole device.

The energy levels in Figure 2 are drawn to fit a frequently employed embodiment of the DSC based on the N719 ruthenium dye (the ditetrabutylammonium salt of N3), the iodide/triiodide as a redox couple, and nanocrystalline anatase films as an electron collector. The ground-state standard redox potential of the N719 as well as that of several other ruthenium complexes and organic sensitizers, measured when the dye is adsorbed to the surface of the nanocrystalline anatase film, is around 1 V against the normal hydrogen electrode (NHE), while the Nernst potential of the triiodide/iodide-based redox electrolyte is close to 0.4 V and the energy of the conduction band edge of anatase at is located at  $-0.5$  V. Neglecting entropy changes during the light absorption and using a 0–0 vibronic transition energy of 1.65 eV, the excited-state redox potential of N719 is derived to be  $-0.65$  eV. Hence, the driving force for electron injection under standard conditions is 0.15 eV. In contrast, the regeneration consumes 0.6 eV, which is clearly excessive. However, using the black dye (N749) instead of N719, the loss is reduced to 0.4 eV because of its 0.2 eV lower ground-state redox potential. Measurements of a series of ruthenium complexes have shown that the minimum driving force required for the near-quantitative interception of the geminate electron recombination with the oxidized sensitizer by oxidation of iodide to triiodide is about 0.2 to 0.3 eV. This relatively high value results from the two-electron character of the iodide oxidation reaction, which passes through I<sub>2</sub><sup>-</sup> radicals as intermediates.

The chemical structures of N3 and the black dye (N749) are shown in Figure 3 together with the spectral response of the photocurrent generated by these sensitizers. The incident photon to current conversion efficiency (IPCE) sometimes referred to also as the “external quantum efficiency” (EQE) is plotted as a function of the excitation wavelength. The IPCE value corresponds to the photocurrent density produced in the external circuit under monochromatic illumination of the cell divided by the photon flux that strikes the cell.

$$\text{IPCE}(\lambda) = \text{LHE}(\lambda)\phi_{\text{inj}}\eta_{\text{coll}} \quad (1)$$

Here,  $\text{LHE}(\lambda)$  is the light-harvesting efficiency for photons of wavelength  $\lambda$ ;  $\phi_{\text{inj}}$  is the quantum yield for electron injection from the excited sensitizer in the conduction band of the semiconductor oxide; and  $\eta_{\text{coll}}$  is the electron collection efficiency. Figure 4 shows that the IPCE reaches close to 80% for both



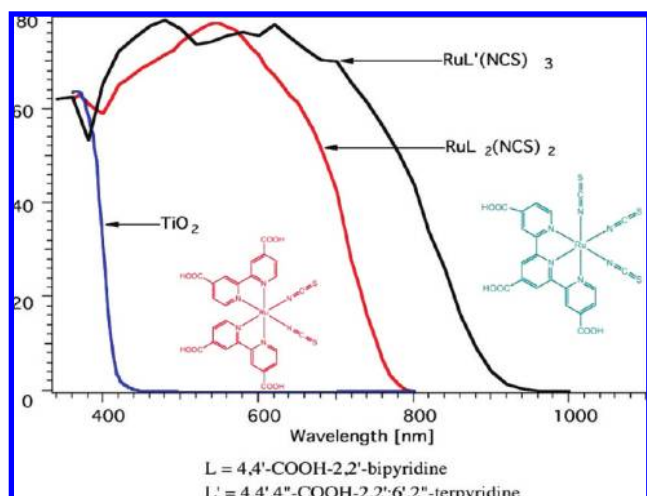


**FIGURE 3.** Incident photon to current conversion efficiency as a function of the wavelength for the standard ruthenium sensitizers N3 (red line), the black dye N749 (black curve), and the blank nanocrystalline TiO<sub>2</sub> film (blue curve). The chemical structure of the sensitizers are shown as insets.

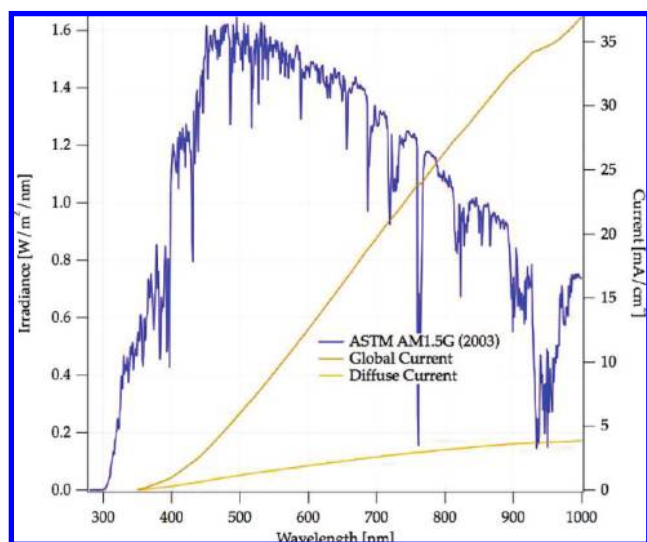


**FIGURE 4.** (Blue curve) Spectral distribution of the intensity for AM 1.5 solar radiation. (Yellow curves)  $J_{sc}$  values for a device converting all incident photons below the absorption onset wavelength into electric current.

sensitizers in the plateau region of the IPCE spectrum. In comparison to the N3 sensitizer, the spectral response of the black dye extends further into the near IR, with its photocurrent onset being around 900 nm instead of 800 nm for the former dye. This corresponds to a band gap of 1.4 eV, which is close to the optimum threshold absorption for single-junction photovoltaic cells. However, for both sensitizers, the IPCE curve rises only gradually from the absorption onset to shorter wavelengths because of the low extinction coefficients of the sensitizers in the longer wavelength range. This behavior results in a very significant loss in photocurrent. For example, the photocurrent density obtained currently with the

N749 (black) dye under standard conditions is close<sup>11,12</sup> to 21 mA/cm<sup>2</sup>, while from Figure 4, the maximum  $J_{sc}$  for a sensitizer with an absorption onset of 900 nm is 33 mA/cm<sup>2</sup>. Even if one concedes an IPCE loss of 10% across the whole spectral absorption domain of the black dye, reducing  $J_{sc}$  to 30 mA/cm<sup>2</sup>, the gain in photocurrent would still boost the overall conversion efficiency of the device by a factor of 1.5 to over 15%. Improving the light harvesting in the 650–900 nm domain is therefore one of the greatest challenges faced by present day research in the DSC field. Even moderate improvements in the photoresponse of the sensitizer in red and near-IR wavelength regions would greatly benefit the conversion efficiency.

### State of the Art Performance of Dye-Sensitized Solar Cells

The overall conversion efficiency of the dye-sensitized cell is determined by the photocurrent density measured at short circuit ( $J_{sc}$ ), the open-circuit photovoltage ( $V_{oc}$ ), the fill factor of the cell (FF), and the intensity of the incident light ( $I_s$ ).

$$\eta_{\text{global}} = J_{sc} V_{oc} \text{FF} / I_s \quad (2)$$

The fill factor can assume values between 0 and 1 and is defined by the ratio of the maximum power ( $P_{\text{max}}$ ) of the solar cell divided by the open-circuit voltage ( $V_{oc}$ ) and the short-circuit current ( $I_{sc}$ ).

$$\text{FF} = P_{\text{max}} / (I_{sc} V_{oc}) \quad (3)$$

$P_{\text{max}}$  is the product of the photocurrent and photovoltage at the voltage where the power output of the cell is maximal. The value of the fill factor reflects the extent of electrical (Ohmic) and electrochemical (overvoltage) losses occurring during operation of the DSC. Increasing the shunt resistance and decreasing the series resistance as well as reducing the overvoltage for diffusion and electron transfer will lead to higher fill factors, thus resulting in greater efficiency and pushing the output power of the cell closer toward its theoretical maximum.

Under full sunlight, corresponding to the standard air mass 1.5 global (AM 1.5 G) spectral distribution and an intensity  $I_s = 1000 \text{ W/cm}^2$ ,  $J_{sc}$  values ranging from 16 to 22 mA/cm<sup>2</sup> are reached with state of the art ruthenium sensitizers, while the  $V_{oc}$  attains 0.7–0.86 V and typical values for the fill factor are 0.65–0.8. Note that the fill factor of a DSC is affected by the transfer coefficient  $\beta$  for the electron transfer from TiO<sub>2</sub> to the electrolyte, whose rate shows exponential voltage dependence, following a Tafel law.<sup>12</sup> For a given  $V_{oc}$ , the larger the  $\beta$  value, the better the fill factor. Theoretically,  $\beta$  should be 1

for electron transfer from a semiconductor to a solution redox couple, but smaller values are usually observed because of the participation of surface states in the interfacial charge transfer, whose energy levels lie below the conduction band of TiO<sub>2</sub>. A larger  $\beta$  value can be associated with a shallower distribution of these defect states.<sup>12</sup>

Until recently, the photovoltaic performance of the black N749 dye was superior to all other known charge-transfer sensitizers. In 2006, a certified conversion efficiency of 11.1% was reached with this dye.<sup>11</sup> The short-circuit current of this device under standard AM 1.5 sunlight was 20.9 mA/cm<sup>2</sup>; the open-circuit voltage was 0.736 V; and the fill factor was 0.722.

The advantage of the black panchromatic sensitizer is apparent from Figure 4, where the photocurrent density is plotted as a function of the wavelength of the absorption onset assuming that all photons whose energy is above this threshold are converted into electric current. The blue curve shows the spectral distribution of the intensity for AM 1.5 solar radiation. A bathochromic extension of the spectral response by 100 nm in the 600–900 nm wavelength range increases the maximal  $J_{sc}$  by ca. 7 mA/cm<sup>2</sup>. Because the IPCE values for the N3 and N749 sensitizers in Figure 3 reach only 70–80%, their  $J_{sc}$  values are expected to differ by about 4–5 mA/cm<sup>2</sup>, in keeping with the experimental observations.

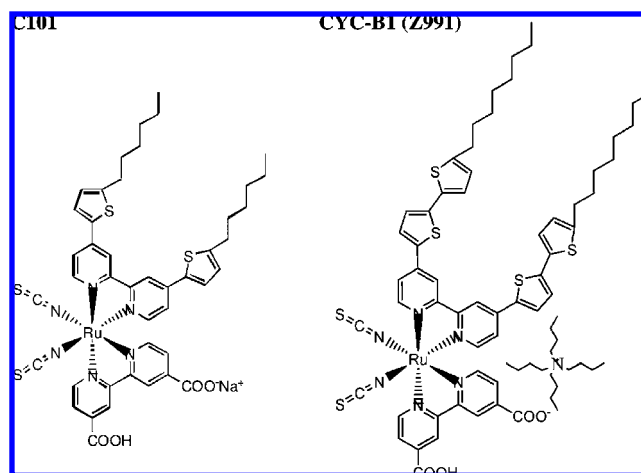
The precise  $J_{sc}$  value produced by the solar cell in AM 1.5 solar light can be derived by integrating the IPCE spectra in Figure 3 over the spectral distribution of the standard AM 1.5 solar photon flux ( $I_s$ ) represented in Figure 4

$$J_{sc} = \int e \text{IPCE}(\lambda) I_s(\lambda) d\lambda \quad (4)$$

where  $e$  is the elementary charge. Performing this integration is important to confirm the  $J_{sc}$  values determined with a solar simulator. Any discrepancy between the measured  $J_{sc}$  value and that derived from the IPCE spectrum using eq 4 signals a spectral mismatch between the simulator and the true AM 1.5 solar emission, rendering the photocurrents incorrect.

## Recent Efficiency Advances Using New Heteroleptic Ruthenium Complexes

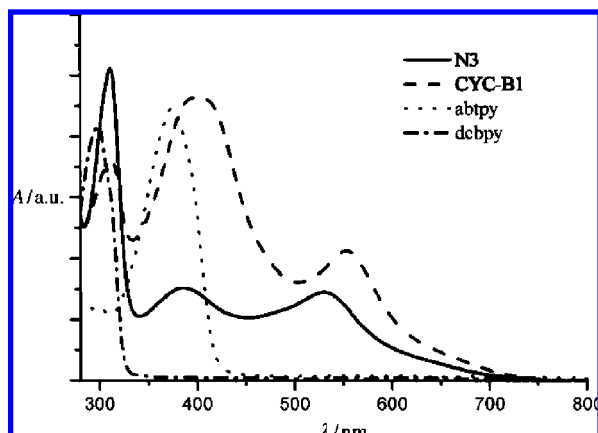
The recent advent of heteroleptic ruthenium complexes endowed with an antenna function has led to striking advances in the performance of the DSC.<sup>14–22</sup> Examples for representatives of this new generation of highly efficient and stable sensitizers are the C101 and CYC-B1 (Z991) dyes, whose structures are shown below. The thiophene moieties attached to the ancillary bipy-ligand enhance the light-harvesting capacity of these complexes by increasing their extinc-



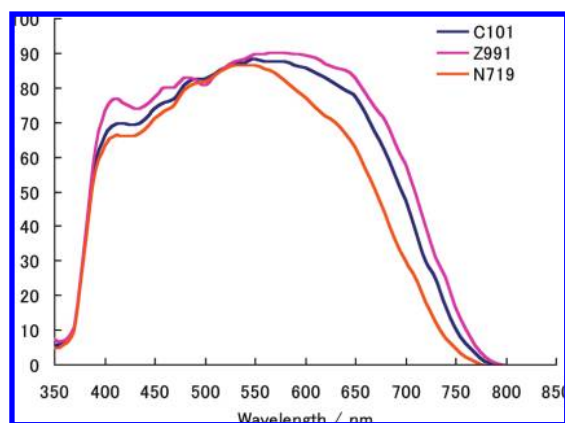
tion coefficient and shifting their spectral response to the red. Figure 5 compares the absorption spectrum of CYC-B1 to that of the N3 dye.<sup>14</sup> The introduction of the alkyl-bis-thiophene moiety produces a strong new band centered at around 410 nm. Borrowing intensity from this transition, the maximum of the metal-to-ligand charge transfer (MLCT) band in the visible region is shifted from 530 to 553 nm and the extinction coefficient is increased from 14 500 to 21 200 M<sup>-1</sup> cm<sup>-1</sup>.

Figure 6 shows the IPCE curves obtained with the N719, C101, and Z991 sensitizers using the same nanocrystalline TiO<sub>2</sub> films and an iodide/triiodide-based redox electrolyte of identical composition. Introducing the thiophene-substituted bipy ancillary ligands produces a small shift in the onset wavelength of the photocurrent from 775 to 800 nm. However, much more important and beneficial is the steeper rise of the IPCE curve and the higher IPCE values, reaching as much as 90% in the plateau region. For the Z991 sensitizer, the maximum of the IPCE spectrum is at 600 nm, i.e., 50 nm red-shifted from the maximum of the solution spectrum, shown in Figure 5. At 700 nm, where the solution absorption shows a weak tail, the IPCE attained by the Z991 sensitizer is still over 70%. The enhanced red response is likely to arise from lateral  $\pi$ -stacking interactions of the bithiophene groups of adjacent chromophores adsorbed at the TiO<sub>2</sub> surface. If confirmed, this would open up new possibilities to enhance the red and near-IR response of dye-sensitized nanocrystalline oxide films.

On the basis of their favorable IPCE characteristics, these new “supersensitizers” can reach  $J_{sc}$  values matching those obtained with the black dye, even though their photocurrent onset is at a shorter wavelength, i.e., 800 nm instead of 900 nm. The great advantage of the heteroleptic complexes, such as Z991, is that their extinction coefficients are almost 3 times higher than that of N749. This allows for the reduction of the TiO<sub>2</sub> film thickness, resulting in higher  $V_{oc}$  values because of a decrease in the dark current and increase in the electron



**FIGURE 5.** UV/vis absorption spectra of N3, CYC-B1, as well as those of the dicarboxy-bipyridine (dc bpy) and alkylbisthiophene (abtp) ligands in DMF solution..<sup>11</sup>



**FIGURE 6.** IPCE spectra obtained with the three sensitizers N709, C101, and Z991 (CYC-B1) using the same nanocrystalline TiO<sub>2</sub> film and identical redox electrolyte based on the iodide triiodide redox couple. Detailed experimental conditions are provided in refs 14–16. The ordinate of the figure expresses the IPCE values in percent.

concentration. Also, applying thinner films augments the fill factor of the device because of the decrease of the electrolyte resistance and the diffusion overvoltage for triiodide reduction at the counter-electrode. The AM 1.5 solar to electric conversion efficiencies attained with these types of sensitizers has therefore been rising continuously over the last 2 years as new synthetic variants are being introduced,<sup>20</sup> reaching presently 12%. Because these sensitizers are very robust and show excellent stability under exposure to prolonged high temperature and light soaking stress, their prospects of practical applications are very good.

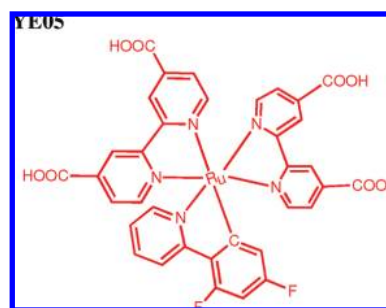
## New Paradigm, Cyclo-Metalated Ruthenium Complexes

Cyclo-metalated ruthenium complexes have emerged recently as a new paradigm in the molecular engineering of sensitizers for solar cell applications. Many attempts had been made

in the past to replace the thiocyanate donor ligands in the series of ruthenium complexes reported above, because the monodentate SCN<sup>-</sup> is believed to be the weakest part of the complex from a chemical stability point of view. However, thus far, these efforts have yielded only limited success, because the conversion efficiency achieved with complexes that do not contain SCN<sup>-</sup> remain well below 10%. A very promising result was obtained recently with the complex YE05, whose structure is shown below.<sup>23</sup> In a standard DSC configuration, this cyclo-metalated complex showed an IPCE spectrum with a maximum of over 80% at 600 nm extending to 800 nm. The significant red shift in the spectral response of the YE05 compared to that of the standard N719 is attributed to the fact that the cyclo-metalated ligand is a stronger donor than the two thiocyanate groups, resulting in a destabilization of the Ru(t<sub>2g</sub>) levels and narrowing of the highest occupied molecular orbital (HOMO)–lowest unoccupied molecular orbital (LUMO) gap of the sensitizer.

Under AM 1.5 standard sunlight, the YE05 produces a short-circuit photocurrent of 17 mA/cm<sup>2</sup>, a V<sub>oc</sub> of 800 mV, and a fill factor of 0.74, corresponding to an overall conversion efficiency of 10.1%. Details of these measurements are shown in Figure 7 along with time-dependent density functional theory (DFT) calculations of the electron density in the LUMO and HOMO of the sensitizer.

The 10% efficiency achieved by the TiO<sub>2</sub> solar cell sensitized by YE05 can be related to the broad range of visible light absorption of the dye. Time-dependent DFT calculations have unraveled the importance of the cyclo-metalated ligand, whose electron-donating property is modulated by the presence of the two fluorine substituents. The role of the fluorine



is to reduce the Lewis basicity of the carbanion in the cyclo-metalated ligand, possibly adjusting the Ru<sup>II</sup>/Ru<sup>III</sup> redox potential at a level where rapid regeneration of the sensitizer by the iodide ion is possible. The presence of the carbanionic ligand stabilizes the Ru<sup>III</sup> state that is generated upon oxidation of the complex during injection of an electron into the conduction band of TiO<sub>2</sub>.



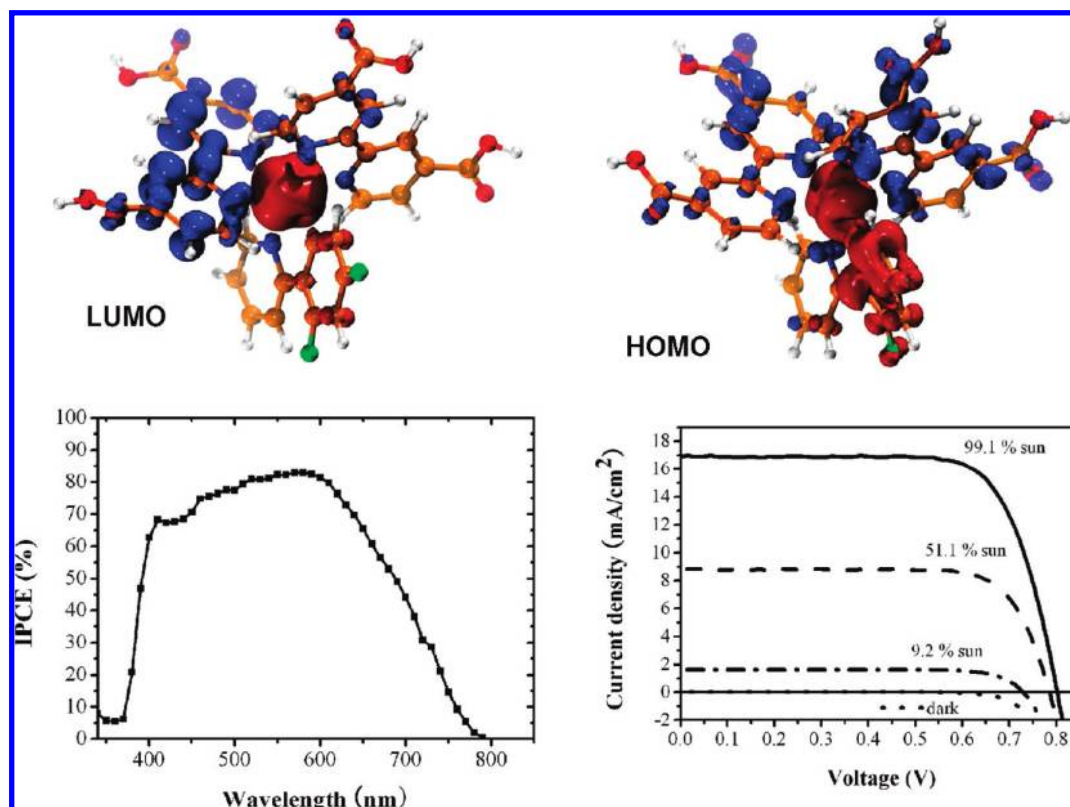
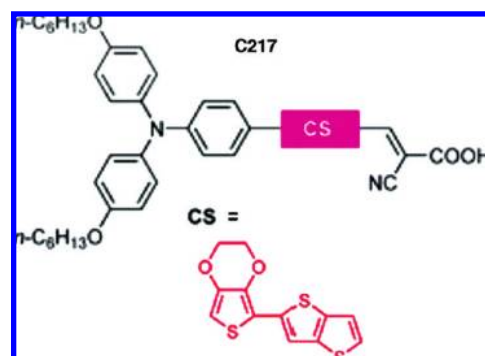


**FIGURE 7.** (Top) Electron density distribution in the HOMO and LUMO involved in the optical excitation of the YE05 sensitizer derived from time-dependent DFT calculations.<sup>20</sup> (Bottom) IPCE spectrum (left) and photocurrent voltage curves (right) under various light intensities of AM 1.5 sunlight. The conversion efficiency obtained at full solar light exposure is 10.1%.

The positive charge is shared by the cyclo-metalated ligand, allowing rapid transfer to the iodide ions in the adjacent electrolyte. The importance of the role of the fluorine substituents in tuning the electron-donating property of the ligand is confirmed by the observation that a sensitizer containing no fluorine on the cyclo-metalated ligand is much less efficient than complex YE05. The absorption spectrum of the YE05 complex is dominated in the visible region by three bands at 406, 486, and 560 nm, which are attributed to MLCT transitions. The lowest energy MLCT band in YE05 is red-shifted by 25 nm when compared to the standard N719 sensitizer, a new band appearing at 486 nm, where the N719 spectrum shows a valley. The striking feature of the complex YE05 is the remarkably high molar extinction coefficient exceeding substantially that of N719 over the whole visible domain. Thus, YE05 emerges as a prototype for thiocyanate-free cyclo-metalated ruthenium complexes, exhibiting remarkable spectral and stability properties. This novel generation of ruthenium complexes appear as a promising class of robust and panchromatic sensitizers enabling greatly enhanced DSC performance.

## Organic Sensitizers

Over the last 2 decades, ruthenium complexes endowed with appropriate ligands and anchoring groups have been by far the preferred choice of charge-transfer sensitizers for mesoscopic solar cells. Recently, however, there has been a surge of interest in organic dyes.<sup>24</sup> As shown in Figure 8, solar to electric power conversion efficiencies have been sharply increasing, reaching 9.5% in 2008 for the indoline dye D205.<sup>25</sup> This rapid development has culminated in the recent report of a 9.8% DSC based on the new sensitizer<sup>26</sup> C217, whose structure is shown below.



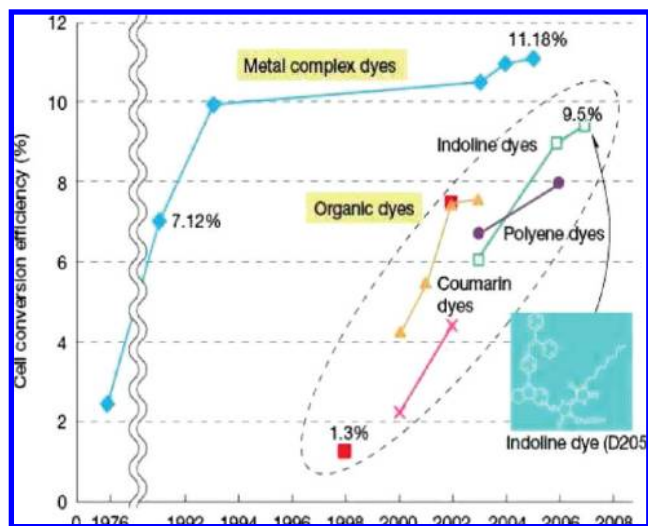


**FIGURE 8.** Evolution of standard AM 1.5 solar to electric power conversion efficiencies for DSCs based on ruthenium complexes and organic dyes (source: Tetsuo Nozawa *Nikkei Electronics Asia*, July 2008).

While the D205 indoline dye is probably not stable enough for use in outdoor photovoltaic devices, other chemically very robust dyes, such as C217, have recently been developed by several groups.<sup>27–31</sup> These dyes contain an electron donor (D) and acceptor (A) moiety, constituted typically by an arylamine and a cyanoacrylate group, respectively, which are connected via one or several thiophene moieties acting as a  $\pi$ -conducting bridge. Structures of this kind will be abbreviated below as D- $\pi$ -A dyes. The sensitizer is attached to the surface of the mesoscopic titania film via the cyanoacrylate group that binds it coordinatively to the surface  $\text{Ti}^{\text{IV}}$  ions. Molecular orbital calculations show the electron density of the HOMO of the sensitizer to be mainly located on the arylamine, while the LUMO is centered at the cyanoacrylate moiety. Hence, during light excitation, electrons are transferred from the triarylamine through the thiophene bridge to the surface-bound cyanoacrylate, producing strong coupling of the excited state wave function with the  $\text{Ti}(3d, t2g)$  orbitals that form the conduction band of titanium dioxide. As a consequence, efficient and rapid electron injection from the excited state of the sensitizer into the conduction band of the oxide can be achieved. Chemically and photochemically robust D- $\pi$ -A dyes have been developed, resisting degradation over 1000 h of light soaking at full solar intensity and elevated temperatures.<sup>26,27,30</sup>

While the photovoltaic results obtained with the current generation of D- $\pi$ -A sensitizers are impressive and encouraging, overall solar to power conversion efficiencies remain still somewhat below the values achieved with ruthenium complexes because of insufficient light absorption above 700 nm. It is therefore important to conceive new sensitizers with

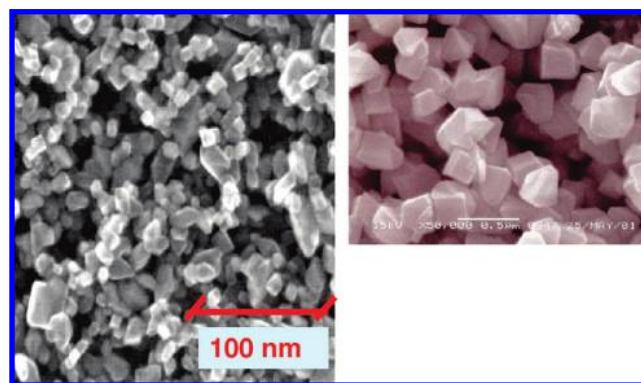


**FIGURE 9.** Scanning electron microscope pictures of a transparent nanocrystalline  $\text{TiO}_2$  film formed by 20 nm sized anatase (left) and 200–400 nm sized anatase light-scattering particles (right).

enhanced spectral response in the red and near-IR regions by designing modified structures of the existing working dyes. With the number of suitable options for dye structures being very large, state of the art theoretical chemical calculations should be employed as a guide for the selection of the most promising candidates for synthesis. The recently developed scaled opposite-spin configuration interaction singles–doubles code, abbreviated as SOS-CIS(D),<sup>31</sup> appears to offer great accuracy in calculating the UV–vis spectra for such novel D- $\pi$ -A sensitizers. This new method is superior to the time-dependent density functional theory (TDDFT) and will assist the experimentalists in the judicious selection of molecular components to engineer the best-performing molecular chromophores for future generation dye-sensitized solar cells.

### Importance of the Nanostructure

The nanocrystalline morphology of the oxide semiconductor film is essential for the efficient operation of the DSC. On a flat surface, a monolayer of dye absorbs at most a small percent of impinging light because it occupies an area that is several hundred times larger than its optical cross-section. Employing a mesoscopic oxide to support the monolayer of a sensitizer allows one to overcome this notorious inefficiency problem. A whole range of nanostructures has been tested thus far, ranging from simple assemblies of nanoparticles to nanorods<sup>32</sup> and nanotubes.<sup>33,34</sup> These studies are motivated by the expectation that the transport of charge carriers along the tubes is more facile than within a random network of nanoparticles, where the electrons have to cross many particle boundaries. Hence, one-dimensional nanostructures should produce a lower diffusion resistance than the nanocrystalline films facilitating the collection of photogenerated charge carriers. Figure 9 shows a scanning electron microscopy picture of a mesoscopic  $\text{TiO}_2$  (anatase) layer. The particles have an



average size of 20 nm, and the facets exposed have mainly (101) orientation, corresponding to the anatase crystal planes with the lowest surface energy (ca. 0.5 J/m<sup>2</sup>).

The light harvesting by the surface-adsorbed sensitizer can be further improved by introducing larger titania particles in the film that scatter light. These are either mixed with or printed on top of the film of 15–30 nm sized TiO<sub>2</sub> nanoparticles. The scattered photons are contained in the film by multiple reflections, increasing their optical path length substantially beyond the film thickness. As a result, the absorption of solar light is enhanced, particularly in the red and near-IR spectral regions, where the currently used ruthenium complexes show only weak light absorption. For example, using 200–400 nm sized anatase particles as light-scattering centers increases the  $J_{sc}$  of N719-based DSCs by as much as 3–4 mA/cm<sup>2</sup> because of the enhanced absorption of red or near-infrared photons.<sup>35</sup> A scanning electron micrograph of such particles is shown on the right side of Figure 9.

Solids containing periodic pore structures that exhibit photonic band gaps also show great promise for enhancing the red response of the DSC.<sup>36</sup> There are benefits from using such photon capture strategies, because they have been shown to enhance the photocurrent response of the DSC, in particular, in the near-IR and red regions of the solar spectrum. The gain in short-circuit photocurrent and overall conversion efficiency achieved by exploiting these optical effects can be as high as 30%.

## Reproducibility of Cell Fabrication and Scale-up

While the DSC can be produced in a relatively simple way in the laboratory without employing a glovebox or high vacuum steps, a rigorous protocol needs to be applied during cell fabrication to achieve high efficiencies in a reproducible manner. By taking the appropriate precautions, relative variations of the efficiency of less than 2–3% can be readily achieved for laboratory cells. Thus, a detailed procedure providing a guide to realize reproducibly cell efficiency values over 10% has been published recently.<sup>37</sup> Reproducible manufacturing of DSC modules on a semi-automated baseline has also been reported.<sup>38</sup> Because of significant industrial up-scaling efforts, the conversion efficiency of DSC modules has been steadily rising over the past few years, with the certified value measurer under AM 1.5 standard conditions reaching currently 8.2%.<sup>39</sup>

## Stability and Commercial Development of the DSC

Long-term stability is a key requirement for all types of solar cells. A vast amount of tests have therefore been carried over the last 15 years to scrutinize the stability of the DSC by both academic and industrial institutions. Most of the earlier work has been reviewed.<sup>40,41</sup> Long-term accelerated light-soaking experiments performed over many thousands of hours under full or even concentrated sunlight have confirmed the intrinsic stability of current DSC embodiments. Stable operation under high-temperature stress at 80–85 °C as well as under damp heat and temperature cycling has been achieved by judicious molecular engineering of the sensitizers with the use of robust and nonvolatile electrolytes, such as ionic liquids,<sup>42</sup> and adequate sealing materials. In the early development stage of the DSC technology, the quality of device sealing was sometimes not appropriate in laboratory test cells, causing leakage of the volatile solvents. Most research groups with longer practical experience, including industrial enterprises, have overcome this by improving the sealing methods. Because of the direct relevance to the manufacturing of commercial products, little is published on these processing issues though. Good results on overall system endurance have been reported for several years, demonstrating excellent stability under accelerated laboratory test conditions. These promising results are presently being confirmed under real outdoor conditions. From these extensive studies, confidence has emerged that the DSCs can match the stability requirements needed to sustain outdoor operation for at least 20 years. This has paved the way for the recent worldwide surge in the industrial development and commercialization of the DSC.<sup>42</sup>

## Summary

The present Account discusses recent research made in molecular photovoltaic cells based on the sensitization of a nanocrystalline wide-band gap semiconductor oxide film by a dye. These cells have now attained efficiencies in the laboratory as well as in the module scale, which render them competitive to other thin-film solar cells. Their low cost and ease of production, avoiding expensive high vacuum steps, should benefit large-scale applications. Impressive stability under both long-term light soaking and high-temperature stress has been reached fostering first industrial applications. These systems will promote the acceptance of renewable energy technologies, not least by setting new standards of convenience and economy.

Support of this work by the Swiss National Science Foundation is gratefully acknowledged.

## BIOGRAPHICAL INFORMATION

**Michael Grätzel** is a Professor at the Ecole Polytechnique de Lausanne and directs the Laboratory of Photonics and Interfaces there. He discovered a new type of solar cell based on dye-sensitized mesoscopic oxide films and pioneered studies of nanocrystalline semiconductor junctions and their use in photoelectrochemical cells for the splitting of water into hydrogen and oxygen by sunlight. He is the author of over 800 publications, 2 books, and inventor of more than 50 patents. His work has been cited over 50 000 times. He has received numerous prestigious awards, including the Harvey Prize (Technion Israel), the Galvani Medal, the Faraday Medal, the Dutch Havinga Award, the Japan Coordination Chemistry Award, the ENI-Italgas Prize, the European Innovation Prize 2000, and the Gerischer Award. He was selected by the Scientific American as one of the 50 top researchers in the world. He received a doctor's degree in Natural Science from the Technical University Berlin and honorary doctor's degrees from the Universities of Hasselt (Belgium), Delft (The Netherlands), Uppsala (Sweden), and Turin (Italy). He is a member of the Swiss Chemical Society and the European Academy of Science and a Fellow of the Royal Society of Chemistry (FRSC) and was elected as a honorary member of the Société Vaudoise des Sciences Naturelles.

## FOOTNOTES

\*To whom correspondence should be addressed. E-mail: michael.gratzel@epfl.ch.

## REFERENCES

- Desilvestro, J.; Grätzel, M.; Kavan, L.; Moser, J. E.; Augustynski, J. Highly efficient sensitization of titanium dioxide. *J. Am. Chem. Soc.* **1985**, *107*, 2988–2990.
- Vlachopoulos, N.; Liska, P.; Augustynski, J.; Grätzel, M. Very efficient visible light energy harvesting and conversion by spectral sensitization of high surface area polycrystalline titanium dioxide films. *J. Am. Chem. Soc.* **1988**, *110*, 1216–1220.
- O'Regan, B.; Grätzel, M. A low-cost, high efficiency solar cell based on dye sensitized colloidal TiO<sub>2</sub> films. *Nature* **1991**, *335*, 737–740.
- Nazeeruddin, Md. K.; Kay, A.; Rodicio, I.; Humphrey-Baker, R.; Müller, E.; Liska, P.; Vlachopoulos, N.; Grätzel, M. Conversion of light to electricity by *cis*-X<sub>2</sub>bis(2,2'-bipyridyl)-4,4'-dicarboxylate)ruthenium(II) charge transfer sensitizer (X = Cl<sup>-</sup>, Br<sup>-</sup>, I<sup>-</sup>, CN<sup>-</sup>, and SCN<sup>-</sup>) on nanocrystalline TiO<sub>2</sub> electrodes. *J. Am. Chem. Soc.* **1993**, *115*, 6382–6390.
- Bach, U.; Lupo, D.; Comte, P.; Moser, J. E.; Weissörtel, F.; Salbeck, J.; Spreitzer, H.; Grätzel, M. Solid state dye sensitized cell showing high photon to current conversion efficiencies. *Nature* **1998**, *395*, 550.
- Grätzel, M. Photoelectrochemical cells. *Nature* **2001**, *414*, 338–344.
- Qin, P.; Linder, M.; Brinck, T.; Boschloo, G.; Hagfeldt, A.; Sun, L. High incident photon-to-current conversion efficiency of p-type dye-sensitized solar cells based on NiO and organic chromophores. *Adv. Mater.* **2009**, *21*, 1–4.
- Nusbaumer, H.; Zakeeruddin, S. M.; Moser, J.-E.; Grätzel, M. *Chem.—Eur. J.* **2003**, *9*, 3756–3763.
- Brugnati, M.; Caramori, S.; Cazzanti, S.; Marchini, L.; Argazzi, R.; Bignozzi, C. A. *Int. J. Photoenergy* **2007**, *2*, 80756/1–80756/10.
- Zhang, Z.; Chen, P.; Murakami, T. N.; Zakeeruddin, S. M.; Grätzel, M. *Adv. Funct. Mater.* **2008**, *18*, 341–346.
- Nazeeruddin, Md. K.; Pechy, P.; Renouard, T.; Zakeeruddin, S. M.; Humphry-Baker, R.; Comte, P.; Liska, P.; Cevey, L.; Costa, E.; Shklover, V.; Spiccia, L.; Deacon, G. B.; Bignozzi, C. A.; Graetzel, M. Engineering of efficient panchromatic sensitizers for nanocrystalline TiO<sub>2</sub>-based solar cells. *J. Am. Chem. Soc.* **2001**, *123*, 1613–1624.
- Chiba, Y.; Islam, A.; Watanabe, Y.; Komiyama, R.; Koide, N.; Han, L. Dye sensitized solar cells with conversion efficiency of 11.1%. *Jan. J. Appl. Phys.* **2006**, *45*, 24–28.
- Wang, Q.; Ito, S.; Graetzel, M.; Fabregat-Santiago, F.; Mora-Sero, I.; Bisquert, J.; Bessho, T.; Imai, H. Characteristics of high efficiency dye-sensitized solar cells. *J. Phys. Chem. B* **2006**, *110*, 25210–25221.
- Chen, C.-Y.; Wu, S.-J.; Wu, C.-G.; Chen, J.-G.; Ho, K.-C. A ruthenium complex with super-high light-harvesting capacity for dye-sensitized solar cells. *Angew. Chem., Int. Ed.* **2006**, *45*, 5822–5825.
- Chen, C.-Y.; Wu, S.-J.; Wu, C.-G.; Chen, J.-G.; Ho, K.-C. A new route to enhance the light-harvesting capability of ruthenium complexes for dye-sensitized solar cells. *Adv. Mater.* **2007**, *19* (22), 3888–3891.
- Chen, C.-Y.; Wu, S.-J.; Wu, C.-G.; Chen, J.-G.; Ho, K.-C. New ruthenium complexes containing oligoalkylthiophene-substituted 1,10-phenanthroline for nanocrystalline dye-sensitized solar cells. *Adv. Funct. Mater.* **2007**, *17* (1), 29–36.
- Gao, F.; Wang, Y.; Zhang, J.; Shi, D.; Wang, M.; Humphry-Baker, R.; Wang, P.; Zakeeruddin, S.-M.; Grätzel, M. A new heteroleptic ruthenium sensitizer enhances the absorptivity of mesoporous titania film for a high efficiency dye-sensitized solar cell. *Chem. Commun.* **2008**, 2635–2637.
- Qin, H.; Wenger, S.; Xu, M.; Gao, F.; Jing, X.; Wang, P.; Zakeeruddin, S.-M.; Grätzel, M. An organic sensitizer with a fused dithienothiophene unit for efficient and stable dye-sensitized solar cells. *J. Am. Chem. Soc.* **2008**, *130* (29), 9202–9203.
- Gao, F.; Wang, Y.; Shi, D.; Zhang, J.; Wang, M.; Jing, X.; Humphry-Baker, R.; Wang, P.; Zakeeruddin, S.-M.; Grätzel, M. Enhance the optical absorptivity of nanocrystalline TiO<sub>2</sub> film with high molar extinction coefficient ruthenium sensitizers for high performance dye-sensitized solar cells. *J. Am. Chem. Soc.* **2008**, *130* (32), 10720–10728.
- Cao, Y.; Bai, Y.; Yu, Q.; Cheng, Y.; Liu, S.; Shi, D.; Gao, F.; Wang, P. Dye-sensitized solar cells with a high absorptivity ruthenium sensitizer featuring a 2-(hexylthio)thiophene conjugated bipyridine. *J. Phys. Chem. C* **2009**, *113*, 6290–6297.
- Abbotto, A.; Barolo, C.; Bellotto, L.; De Angelis, F.; Grätzel, M.; Manfredi, N.; Marini, C.; Fantacci, S.; Yum, J.-H.; Nazeeruddin, Md. K. Electron-rich heteroaromatic conjugated bipyridine based ruthenium sensitizer for efficient dye-sensitized solar cells. *Chem. Commun.* **2008**, DOI: 10.1039/b900208a.
- Choi, H.; Baik, C.; Kim, S.; Kang, M.-S.; Xu, X.; Kang, H. S.; Kang, S.-O.; Ko, J. J.; Nazeeruddin, Md. K.; Grätzel, M. Molecular engineering of hybrid sensitizers incorporating an organic antenna into ruthenium complex and their application in solar cells. *New J. Chem.* **2008**, *32* (12), 2233–2237.
- Bessho, T.; Yoneda, E.; Yum, J.-H.; Guglielmi, M.; Tavernelli, I.; Imai, H.; Rothlisberger, U.; Nazeeruddin, Md. K.; Grätzel, M. New paradigm in molecular engineering of sensitizers for solar cell applications. *J. Am. Chem. Soc.* **2009**, *131* (16), 5930–5934.
- Imahori, H.; Umeyama, T.; Ito, S. Large  $\pi$ -aromatic molecules as potential sensitizers for highly efficient dye-sensitized solar cells. *Acc. Chem. Res.* **2009**, DOI: 10.1021/ar900034t, and references cited therein.
- Ito, S.; Miura, H.; Uchida, S.; Takata, M.; Sumioka, K.; Liska, P.; Comte, P.; Pechy, P.; Grätzel, M. High-conversion-efficiency organic dye-sensitized solar cells with a novel indoline dye. *Chem. Commun.* **2008**, 5194–5196.
- Zhang, G.; Bala, H.; Cheng, Y.; Shi, D.; Lv, X.; Yu, Q.; Wang, P. High efficiency and stable dye-sensitized solar cells with an organic chromophore featuring a binary  $\pi$ -conjugated spacer. *Chem. Commun.* **2009**, 2198–2200.
- Yum, J.-H.; Hagberg, D. P.; Moon, S.-J.; Karlsson, K. M.; Marinado, T.; Sun, L.; Hagfeldt, A.; Nazeeruddin, Md. K.; Grätzel, M. A light-resistant organic sensitizer for solar-cell applications. *Angew. Chem., Int. Ed.* **2009**, *48*, 1576–1580.
- Xu, M.; Li, R.; Pootrakulchote, N.; Shi, D.; Guo, J.; Yi, Z.; Zakeeruddin, S.-M.; Grätzel, M.; Wang, P. Energy-level and molecular engineering of organic D- $\pi$ -A sensitizers in dye-sensitized solar cells. *J. Phys. Chem. C* **2008**, *112* (49), 19770–19776.
- Xu, M.; Wenger, S.; Bala, H.; Shi, D.; Li, Renzhi, Z.-Y.; Zakeeruddin, S.-M.; Grätzel, M.; Wang, P. Tuning the energy level of organic sensitizers for high-performance dye-sensitized solar cells. *J. Phys. Chem. C* **2009**, *113* (7), 2966–2973.
- Choi, H.; Baik, C.; Kang, S. O.; Ko, J.-J.; Kang, M.-S.; Nazeeruddin, Md. K.; Grätzel, M. Highly efficient and thermally stable organic sensitizers for solvent-free dye-sensitized solar cells. *Angew. Chem., Int. Ed.* **2008**, *47* (2), 327–330.
- Rhee, Y. M.; Head-Gordon, M. Scaled second-order perturbation corrections to configuration interaction singles: Efficient and reliable excitation energy methods. *J. Phys. Chem. A* **2007**, *111*, 5314–5326.
- Galoppini, E.; Rochford, J.; Chen, H.; Saraf, G.; Lu, Y.; Hagfeldt, A.; Boschloo, G.

- Fast electron transport in metal organic vapor deposition grown dye-sensitized ZnO nanorod solar cells. *J. Phys. Chem. B* **2006**, *110*, 16159–16161.
- 33 Shankar, K.; Bandara, J.; Paulose, M.; Wietasch, H.; Varghese, O. K.; Mor, G. K.; LaTempa, T. J.; Thelakkat, M.; Grimes, C. A. Highly efficient solar cells using TiO<sub>2</sub> nanotube arrays sensitized with a donor-antenna dye. *Nano Lett.* **2008**, *8*, 1654–1659.
- 34 Macak, J. M.; Ghicov, A.; Hahn, R.; Tsuchiya, H.; Schmuki, P. Photoelectrochemical properties of N-doped self-organized titania nanotube layers with different thicknesses. *J. Mater. Res.* **2006**, *21*, 2824–2828.
- 35 Rothenberger, G.; Comte, P.; Grätzel, M. A contribution to the optical design of dye-sensitized nanocrystalline solar cells. *Sol. Energy Mater. Sol. Cells* **1999**, *58*, 321–336.
- 36 Colodrero, S.; Mihi, A.; Haggman, L.; Ocana, M.; Boschloo, G.; Hagfeldt, A.; Miguez, H. Porous one-dimensional photonic crystals improve the power-conversion efficiency of dye-sensitized solar cells. *Adv. Mater.* **2009**, *21*, 764–770.
- 37 Ito, S.; Murakami, T. N.; Comte, P.; Liska, P.; Grätzel, C.; Nazeeruddin, Md. K.; Grätzel, M. Fabrication of thin film dye sensitized solar cells with solar to electric power conversion efficiency over 10%. *Thin Solid Films* **2008**, *516*, 4613–4619.
- 38 Späth, M.; Sommeling, P. M.; van Roosmalen, J. A. M.; Smit, H. J. P.; van der Burg, N. P. G.; Mahieu, D. R.; Bakker, N. J.; Kroon, J. M. Reproducible manufacturing of dye-sensitized solar cells on a semi-automated baseline. *Progr. Photovoltaics* **2003**, *11*, 207–220.
- 39 Han, L.; Fukui, A.; Chiba, Y.; Islam, A.; Komiya, R.; Fuke, N.; Koide, N.; Yamanaka, R.; Shimizu, M. Integrated dye-sensitized solar cell module with conversion efficiency of 8.2%. *Appl. Phys. Lett.* **2009**, *94*, 013305/1–013305/3.
- 40 Lenzmann, F. O.; Kroon, J. M. Recent advances in dye-sensitized solar cells. *Adv. OptoElectron.* **2007**, 65073/1–65073/10.
- 41 Grätzel, M. Recent applications of nanoscale materials: Solar cells. *Nanostructured Materials for Electrochemical Energy Production and Storage*; Leite, R. E., Ed.; Springer: New York, 2008; Chapter 1.
- 42 Third International Conference on the Industrialization of Dye Sensitizer Solar Cells, (DSC-IC 3), Nara, Japan, April 2009.